Supplementary Methods

Diffusion tensor image processing

A custom script was used to process the DTI data by wrapping previously published algorithms as described below (script available upon request). DTI data were visually controlled for artifacts. If repeated sequences were not possible for images with low quality, the data were discarded and excluded (**Supplementary Figure 1**). Brain masks were created using the *BET* command in FSL and then revised with morphological operations, as well as manual corrections.

A separate step using *topup* to correct susceptibility induced distortions was skipped in our study as all B0 images and diffusion-weighted frames were acquired using identical antero-posterior phase encoding directions. Spurious image distortions that originated from a combination of eddy currents and real head movement were corrected with the CUDA 8.0 implementation of the eddy command in the FSL software library (version 6.0) with the following parameters: 4 standard deviations as criterion for classifying a slice as outlier (ol_nstd=4), 10 slice to volume iterations (s2v_niter=10), 6 smoothing iterations, during which a filter width of 10, 6, 4, 2, 0, 0 mm for each subsequent smoothing iterations was used. Next, FA and mean diffusivity (MD) maps were calculated by running the *dtifit* command in FSL on the motion corrected DTI dataset; tensors were fitted with a weighted least squared algorithm. DTI data were further processed by the Bayesian multi-fiber estimation method BedpostX (CUDA 8.0 implementation for FSL 6.0), estimating up to 3 fiber populations per voxel (Hernandez *et al.* 2013).

Graph theory parameters

Global and nodal efficiency

The networks ability to transfer information in parallel was quantified by calculating the weighted global efficiency, which is the reciprocal of the harmonic mean of the shortest weighted path length. Networks that have a short average shortest path length between two nodes are considered topologically integrated and efficient (Latora et al. 2001). Global efficiency for a weighted graph G was calculated based on the following equation

$$E_{global}(G) = \frac{1}{N(N-1)} \sum_{i \neq j \in G} \frac{1}{d_{i,j}}$$

where N is the total number of nodes in the network G; $d_{i,j}$ is the weighted shortest paths length between nodes i and j (Latora et al. 2003). Accordingly, weighted nodal efficiency was calculated as nodal counterpart of the weighted global efficiency. Nodal efficiency quantifies the integration of a specific node with all other nodes in the network. It is the normalized sum of the inverse of the shortest path length $d_{i,j}$ of a specific node i to all other nodes (Latora et al. 2003).

$$E_{nodal}(i) = \frac{1}{N-1} \sum_{j \in G} \frac{1}{d_{i,j}}$$

We expect global and nodal efficiency to increase during neonatal brain development (Cao et al. 2017).

Local efficiency

Local efficiency as opposed to nodal efficiency quantifies the integration of a specific node within a subgraph G_i, encompassing all nodes that are immediate neighbours of the node (Latora *et al.* 2001, Latora *et al.* 2003). Thus, local efficiency is a measure of structural segregation.

$$E_{local}(i) = \frac{1}{N} \sum_{i \in G} E_{global}(G_i)$$

The average local efficiency across all nodes serves as global measure of the local efficiency of a network. Local efficiency is expected to decrease during neonatal brain development (Cao *et al.* 2017).

Strength

By summing the edge weights ($w_{i,j}$) of all edges connected to a node, nodal strength was calculated. Global strength was measured by averaging the strength of all nodes in the network (Barrat et al. 2004) and is expected to increase with brain network development.

$$s_i = \sum_{j \in G} w_{i,j}$$

Transitivity

Transitivity, which is sometimes also referred to as clustering coefficient, quantifies the probability that the nodes j and h, which are directly connected to node i are also directly connected with each other (Barrat et al. 2004). For global transitivity the number of connected triangles is divided by the number of connected triplets. For the nodal counterpart the weighted transitivity was calculated following the generalization by Barrat et al. (Barrat et al. 2004). $w_{i,h}$

is the edge weight; s_i is the sum of all neighboring edge weights; k_i is the vertex degree, i.e. the number of all edges connected to that node; a_{ij} denotes the element in the adjacency matrix.

$$transitivity_i = \frac{1}{s_i(k_i - 1)} \sum_{j,h} \frac{w_{ij} + w_{ih}}{2} a_{ij} a_{ih} a_{jh}$$

Transitivity as measure of structural segregation is expected to decrease with brain network development (Cao et al. 2017).

Supplementary Figure 1
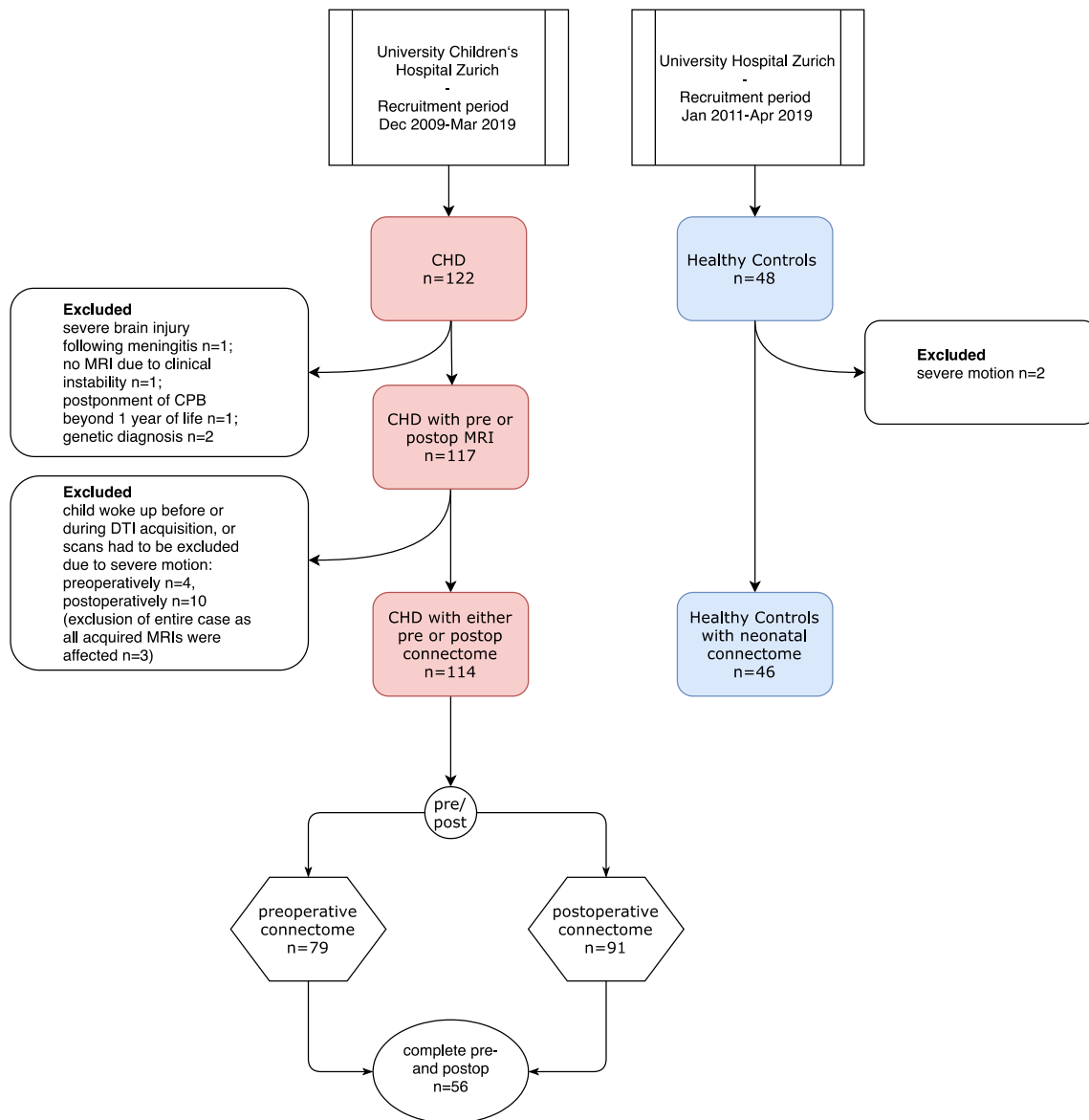
Supplementary Figure 1 Flow chart of included subjects and available connectomes.

Supplementary Table 1

Lobe	Region	Threshold*	ß*	SE*	95% CI*	P_{fdr}*	Amtpc	Acrit
Controls > CHD								
Nodal efficiency								
Frontal	SFGdor.L	0,18	0,029	0,0054	[0.017; 0.042]	1,6E-06	0,48	0,25
	SFGdor.R	0,18	0,028	0,0054	[0.016; 0.04]	0,000003	0,38	0,25
	ORBsup.L	0,15	0,038	0,0068	[0.023; 0.053]	1,2E-06	0,71	0,25
	ORBsup.R	0,08	0,029	0,006	[0.016; 0.043]	0,000021	0,63	0,25
	ORBmid.L	0,11	0,074	0,012	[0.046; 0.1]	2,4E-07	0,89	0,25
	OLF.L	0,18	0,02	0,0043	[0.01; 0.03]	0,000014	0,27	0,25
	OLF.R	0,18	0,022	0,0041	[0.013; 0.031]	1,9E-06	0,45	0,25
	SFGmed.L	0,15	0,035	0,007	[0.019; 0.051]	5,1E-06	0,29	0,25
Insula	INS.L	0,18	0,022	0,0044	[0.013; 0.032]	3,3E-06	0,69	0,25
	INS.R	0,18	0,026	0,0041	[0.016; 0.035]	1,5E-07	0,69	0,25
Limbic	ACG.R	0,18	0,027	0,005	[0.015; 0.038]	1,9E-06	0,59	0,25
	DCG.L	0,18	0,026	0,0046	[0.016; 0.037]	6,5E-07	0,43	0,25
	DCG.R	0,18	0,028	0,005	[0.017; 0.039]	8,8E-07	0,43	0,25
	PCG.L	0,17	0,032	0,0054	[0.02; 0.045]	4,3E-07	0,71	0,25
	PCG.R	0,18	0,042	0,0063	[0.028; 0.056]	3,2E-08	0,88	0,25
Occipital	CAL.R	0,14	0,021	0,0044	[0.011; 0.031]	0,000013	0,36	0,25
	MOG.R	0,13	0,026	0,0062	[0.012; 0.04]	0,000068	0,25	0,25
	IOG.R	0,13	0,038	0,007	[0.022; 0.054]	1,7E-06	0,52	0,25
	FFG.R	0,07	0,032	0,0074	[0.016; 0.049]	0,00015	0,62	0,25
Parietal	ANG.R	0,18	0,023	0,0041	[0.014; 0.032]	8,8E-07	0,31	0,25
SCGM	PUT.L	0,18	0,021	0,0043	[0.011; 0.031]	7,2E-06	0,37	0,25
	PUT.R	0,18	0,022	0,0046	[0.012; 0.033]	7,5E-06	0,41	0,25
Temporal	HES.L	0,18	0,021	0,0046	[0.011; 0.031]	0,000013	0,27	0,25
	STG.L	0,18	0,02	0,0042	[0.01; 0.029]	0,000009	0,27	0,25
	ITG.R	0,13	0,025	0,0053	[0.013; 0.037]	0,000015	0,34	0,25
Strength								
Frontal	ORBsup.L	0,13	1,6	0,32	[0.89; 2.4]	0,00003	0,86	0,21
	ORBsup.R	0,1	1,4	0,3	[0.74; 2.1]	0,000072	0,65	0,21
	ORBmid.L	0,18	1,4	0,29	[0.73; 2]	0,000069	0,74	0,21
	ORBmid.R	0,18	1,5	0,33	[0.7; 2.2]	0,00013	0,71	0,21
	SFGmed.L	0,15	1,3	0,26	[0.74; 1.9]	0,000027	0,51	0,21
	SFGmed.R	0,03	1,2	0,25	[0.68; 1.8]	0,000037	0,23	0,21
Limbic	PCG.R	0,18	4,4	0,66	[2.9; 5.9]	3,3E-08	0,84	0,21
Occipital	IOG.R	0,17	1,3	0,28	[0.66; 1.9]	0,000084	0,41	0,21
CHD > Controls								
Transitivity								
Frontal	SFGdor.L	0,13	0,13	0,025	[0.072; 0.19]	5,1E-06	0,37	0,16
	SFGdor.R	0,11	0,15	0,035	[0.075; 0.23]	0,00006	0,34	0,16
Insula	INS.R	0,07	0,15	0,031	[0.08; 0.22]	0,000031	0,49	0,16

	ACG.L	0,14	0,098	0,022	[0.048; 0.15]	0,000038	0,21	0,16
	DCG.L	0,13	0,067	0,011	[0.042; 0.092]	1,9E-07	0,5	0,16
	DCG.R	0,14	0,064	0,012	[0.035; 0.092]	4,9E-06	0,41	0,16
Limbic	PCG.L	0,15	0,11	0,02	[0.066; 0.16]	0,000001	0,57	0,16
	PCG.R	0,15	0,14	0,023	[0.085; 0.19]	2,3E-07	0,41	0,16
	HIP.L	0,16	0,06	0,011	[0.035; 0.086]	0,000002	0,21	0,16
	HIP.R	0,05	0,08	0,029	[0.013; 0.15]	0,013	0,45	0,16
SCGM	PAL.R	0,14	0,091	0,021	[0.044; 0.14]	0,000038	0,17	0,16
Local efficiency								
	PreCG.L	0,03	0,94	0,2	[0.49; 1.4]	0,00023	0,23	0,14
	PreCG.R	0,04	1	0,23	[0.48; 1.5]	0,00053	0,15	0,14
Frontal	SFGdor.L	0,13	0,63	0,14	[0.32; 0.94]	0,00002	0,28	0,14
	SFGdor.R	0,11	0,71	0,15	[0.38; 1]	0,000019	0,41	0,14
	SMA.R	0,09	0,81	0,19	[0.37; 1.3]	0,00019	0,34	0,14
Insula	INS.L	0,04	0,52	0,14	[0.2; 0.84]	0,0036	0,5	0,14
	INS.R	0,06	0,67	0,14	[0.34; 0.99]	0,00011	0,74	0,14
	ACG.L	0,14	0,59	0,11	[0.34; 0.84]	0,000002	0,31	0,14
	DCG.L	0,06	0,53	0,11	[0.27; 0.78]	0,00011	0,65	0,14
	DCG.R	0,09	0,45	0,084	[0.25; 0.64]	0,000013	0,59	0,14
	PCG.L	0,18	0,42	0,069	[0.26; 0.58]	2,8E-07	0,58	0,14
Limbic	PCG.R	0,15	0,47	0,076	[0.29; 0.64]	1,5E-07	0,41	0,14
	HIP.L	0,06	0,42	0,12	[0.15; 0.69]	0,0017	0,42	0,14
	HIP.R	0,05	0,53	0,12	[0.26; 0.8]	0,00049	0,7	0,14
	PHG.L	0,06	0,42	0,16	[0.052; 0.78]	0,018	0,29	0,14
	AMYG.L	0,15	0,6	0,13	[0.3; 0.9]	0,00002	0,2	0,14
	CUN.L	0,18	0,36	0,07	[0.2; 0.51]	1,7E-06	0,19	0,14
Occipital	LING.L	0,14	0,5	0,1	[0.26; 0.73]	7,9E-06	0,2	0,14
	SOG.R	0,1	0,59	0,17	[0.2; 0.99]	0,0017	0,14	0,14
	PoCG.R	0,03	0,64	0,2	[0.19; 1.1]	0,012	0,3	0,14
	SMG.R	0,12	0,71	0,19	[0.27; 1.1]	0,00063	0,19	0,14
Parietal	PCUN.L	0,08	0,43	0,11	[0.19; 0.68]	0,00029	0,18	0,14
	PCUN.R	0,03	0,38	0,16	[0.018; 0.75]	0,049	0,36	0,14
	PCL.L	0,04	0,92	0,2	[0.47; 1.4]	0,00018	0,28	0,14
	CAU.R	0,08	0,5	0,12	[0.23; 0.78]	0,00025	0,32	0,14
	PUT.L	0,04	0,63	0,1	[0.4; 0.87]	4,5E-07	0,59	0,14
	PUT.R	0,05	0,45	0,097	[0.23; 0.67]	0,00037	0,52	0,14
SCGM	PAL.L	0,08	0,62	0,13	[0.31; 0.92]	0,000064	0,35	0,14
	PAL.R	0,14	0,48	0,078	[0.3; 0.65]	1,3E-07	0,43	0,14
	THA.L	0,14	0,34	0,062	[0.2; 0.48]	1,1E-06	0,51	0,14
	THA.R	0,06	0,38	0,084	[0.19; 0.57]	0,00014	0,5	0,14
	HES.L	0,04	0,45	0,2	[-0.0028; 0.89]	0,05	0,23	0,14
Temporal	MTG.R	0,05	0,55	0,16	[0.17; 0.92]	0,0044	0,18	0,14
	ITG.L	0,18	0,46	0,082	[0.27; 0.64]	5,3E-07	0,16	0,14
Strength								
SCGM	THA.L	0,04	1,6	0,31	[0.92; 2.3]	0,000029	0,24	0,23

	THA.R	0,09	1,6	0,32	[0.92; 2.4]	0,000051	0,48	0,23

Supplementary Table 1 Significant nodal level differences between preoperative CHD neonates and healthy controls as revealed by MTPC. As two one-sided tests were performed to determine the direction of the effects, results are grouped by the contrast "Controls > CHD" or "CHD > Controls". *Threshold indicates the cost threshold at which the strongest *ß coefficient was observed. Statistical parameters are given for that threshold. *P_{fdr} is the threshold-specific P-value corrected for multiple comparison across all 90 ROIs by means of the Benjamini Hochberg procedure. Amtpc and Acrit denote the results of the overall MTPC comparison across the whole range of thresholds. SCGM, subcortical gray matter.

Supplementary Table 2

Abbreviation	Name	Lobe
PreCG	Precentral gyrus	Frontal
SFGdor	Superior frontal gyrus (dorsolateral)	Frontal
ORBsup	Superior frontal gyrus (orbital part)	Frontal
MFG	Middle frontal gyrus	Frontal
ORBmid	Middle frontal gyrus (orbital part)	Frontal
IFGoperc	Inferior frontal gyrus (opercular part)	Frontal
IFGtriang	Inferior frontal gyrus (triangular part)	Frontal
ORBinf	Inferior frontal gyrus (orbital part)	Frontal
ROL	Rolandic operculum	Frontal
SMA	Supplementary motor area	Frontal
OLF	Olfactory cortex	Frontal
SFGmed	Superior frontal gyrus (medial)	Frontal
ORBsupmed	Superior frontal gyrus (medial orbital)	Frontal
REC	Rectus gyrus	Frontal
INS	Insula	Insula
ACG	Anterior cingulate and paracingulate gyri	Limbic
DCG	Median cingulate and paracingulate gyri	Limbic
PCG	Posterior cingulate gyrus	Limbic
HIP	Hippocampus	Limbic
PHG	Parahippocampal gyrus	Limbic
AMYG	Amygdala	Limbic
CAL	Calcarine fissure and surrounding cortex	Occipital
CUN	Cuneus	Occipital
LING	Lingual gyrus	Occipital
SOG	Superior occipital gyrus	Occipital
MOG	Middle occipital gyrus	Occipital
IOG	Inferior occipital gyrus	Occipital
FFG	Fusiform gyrus	Occipital
PoCG	Postcentral gyrus	Parietal
SPG	Superior parietal gyrus	Parietal
IPL	Inferior parietal, supramarginal and angular gyri	Parietal
SMG	Supramarginal gyrus	Parietal
ANG	Angular gyrus	Parietal
PCUN	Precuneus	Parietal
PCL	Paracentral lobule	Parietal
CAU	Caudate nucleus	SCGM
PUT	Lenticular nucleus, putamen	SCGM
PAL	Lenticular nucleus, pallidum	SCGM
THA	Thalamus	SCGM
HES	Heschl gyrus	Temporal
STG	Superior temporal gyrus	Temporal
TPOsup	Temporal pole: superior temporal gyrus	Temporal
MTG	Middle temporal gyrus	Temporal

TPOmid	Temporal pole: middle temporal gyrus	Temporal
ITG	Inferior temporal gyrus	Temporal

Supplementary Table 2 List of node abbreviations parcellated with the Automated Anatomical Labeling. Abbreviations are appended by **.L** for left hemispheric and **.R** for right hemispheric regions.

References

Barrat, A., M. Barthelemy, R. Pastor-Satorras and A. Vespignani (2004). "The architecture of complex weighted networks." <u>Proc Natl Acad Sci U S A</u> **101**(11): 3747-3752.

Cao, M., H. Huang and Y. He (2017). "Developmental Connectomics from Infancy through Early Childhood." <u>Trends Neurosci</u> **40**(8): 494-506.

Hernandez, M., G. D. Guerrero, J. M. Cecilia, J. M. Garcia, A. Inuggi, S. Jbabdi, T. E. Behrens and S. N. Sotiropoulos (2013). "Accelerating fibre orientation estimation from diffusion weighted magnetic resonance imaging using GPUs." <u>PLoS One</u> **8**(4): e61892.

Latora, V. and M. Marchiori (2001). "Efficient behavior of small-world networks." <u>Phys Rev Lett</u> **87**(19): 198701.

Latora, V. and M. Marchiori (2003). "Economic small-world behavior in weighted networks." <u>European Physical Journal B</u> **32**(2): 249-263.